Supporting Information for

Solution processed 1D polymer/SWCNT composite arrays for high-performance field effect transistors

Xiaoyu Fan,‡[a] Jingrun Yang,‡[e] Bo Lei, [c] Zhenghao Yang,[d] Pengda Che,[a] Hanfei Gao,[bg] Yun Liu,*[a] Jiangang Feng,[f] Yuchen Wu[b] and Lei Jiang[abg]

[a]Key Laboratory of Bio-inspired Smart Interfacial Science and Technology of Ministry of Education, School of Chemistry, Beihang University, Beijing 100191, P. R. China.

[b]Key Laboratory of Bio-inspired Materials and Interfacial Science, Technical Institute of Physics and Chemistry, Chinese Academy of Sciences, Beijing 100190, P. R. China.

[c]Haidian Maternal & Child Health Hospital, Beijing 100083, China.

[d]Department of Materials Science and Engineering, College of Engineering, Peking University, Beijing 100871, P. R. China.

[e]Department of Dermatology, the First Medical Center of Chinese PLA General Hospital, Beijing, China.

[f]Division of Physics and Applied Physics, School of Physical and Mathematical Sciences, Nanyang Technological University, Singapore 637371, Singapore.

[g]*Ji Hua Laboratory, Foshan 528000, Guangdong, P. R. China*

*E-mail: yunliu@buaa.edu.cn

‡These authors contributed equally to this work.

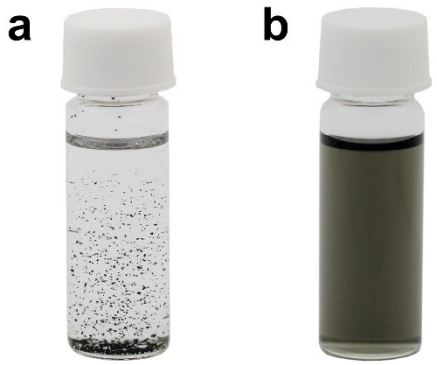

Figure S1. Optical images of pristine SWCNT and PBTTT/SWCNT composite. The polymer wrapped around the SWCNT provides a good dispersibility of the composites. a) SWCNT suspension with poor solubility. b) The homogeneous dispersion of PBTTT/SWCNT composite in DMF.

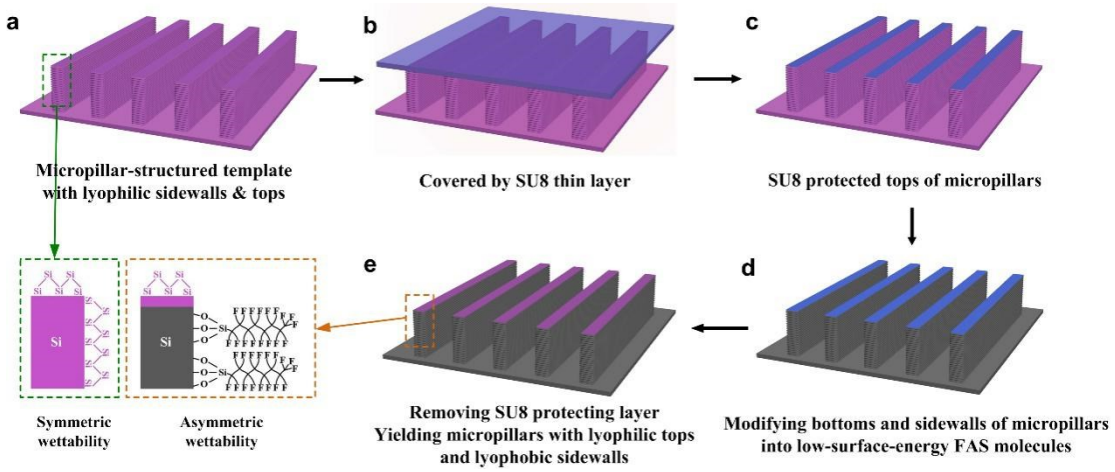

Figure S2. Selective FAS modification of the micropillar-structured template to generate lyophilic tops & lyophobic sidewalls. a) Both tops and sidewalls of the template are lyophilic at the preliminary state. b) A flat substrate covered with a thin layer of SU8 was pressed onto the pillar tops of the template. c) After peeling off the flat substrate, the SU8 protecting layer was leaved on the pillar tops. d) Modification of the top-protected micropillar-structured template with low surface energy heptadecafluorodecyltrimethoxysilane (FAS) molecules. e) Generation of micropillars with asymmetric wettability (lyophilic tops and lyophobic sidewalls) after the removel of SU8 protecting layer by acetone.

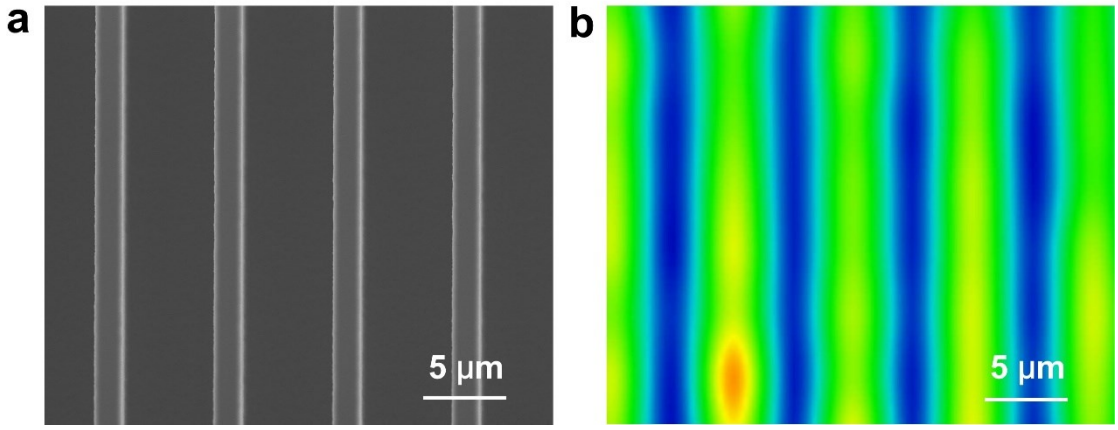

Figure S3. Selective FAS modification of the micropillar-structured template confirmed by Raman mapping. a) SEM image of the selected modified micropillar-structured template. No obvious morphologic change can be observed on the micropillars after modification. b) Raman mapping image of the template with lyophilic tops & lyophobic sidewalls. Strong Raman signal of FAS can be detected at the pillar gap regions (blue regions), whereas nearly no signal can be detected at the top regions (green regions).

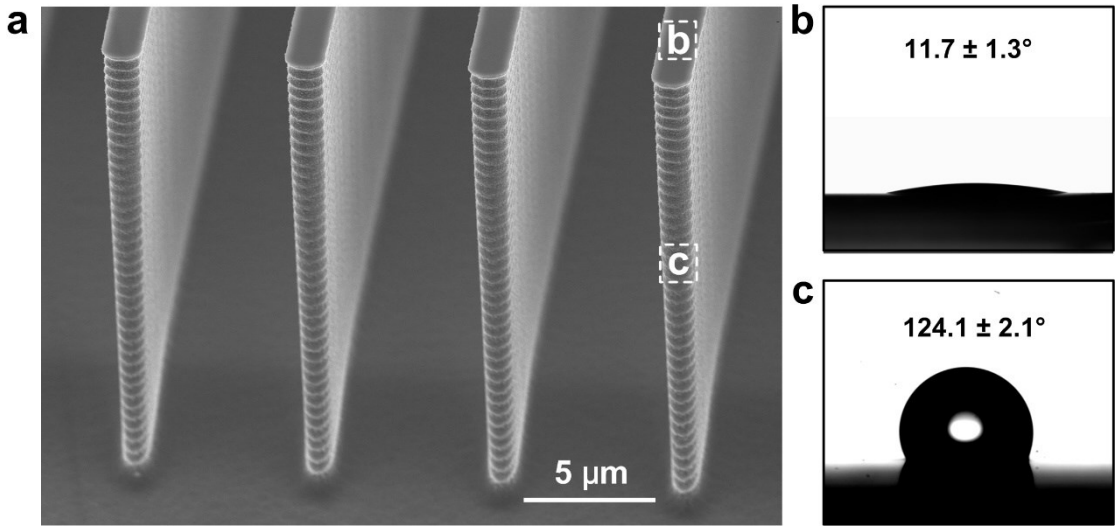

Figure S4. Morphology and wettability measurement of the selective FAS modified template. a) A representative SEM image of the selective FAS modified line-pillar structured template with the width of 2 µm, separation of 5 µm and depth of 20 µm. b) Contact angle (CA) of DMF at the top regions with a low CA of 11.7 ± 1.3^{o}, whereas at the sidewall regions with a high CA of 124.1 ± 2.1^{o}, illustrating the lyophilic tops and lyophobic sidewalls of the template after selective FAS modification.

Figure S5. A hydrophilic flat substrate with a CA of 6.8 ± 1.1° towards DMF.

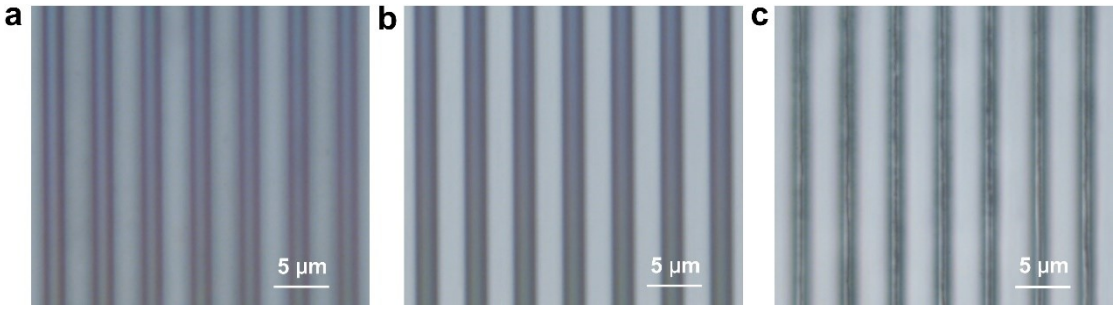

Figure S6. Restricted dewetting and assembly process upon the pillar top regions. a-c) Top-view optical images of the whole dewetting and assembly process under the bright field. 1D π-conjugated PBTTT/SWCNT composite arrays were assembled on top regions successfully.

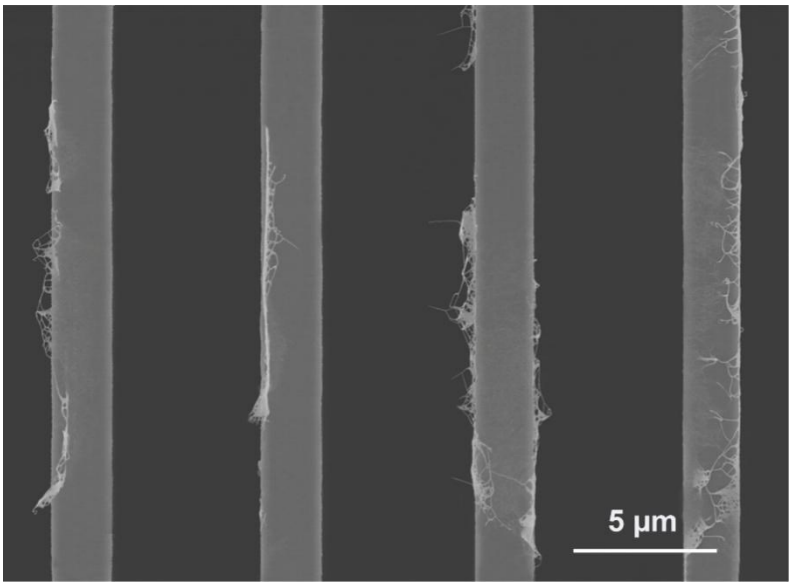

Figure S7. Random positioning of SWCNT on both pillar tops and sidewalls with the symmetric-wettability micropillars.

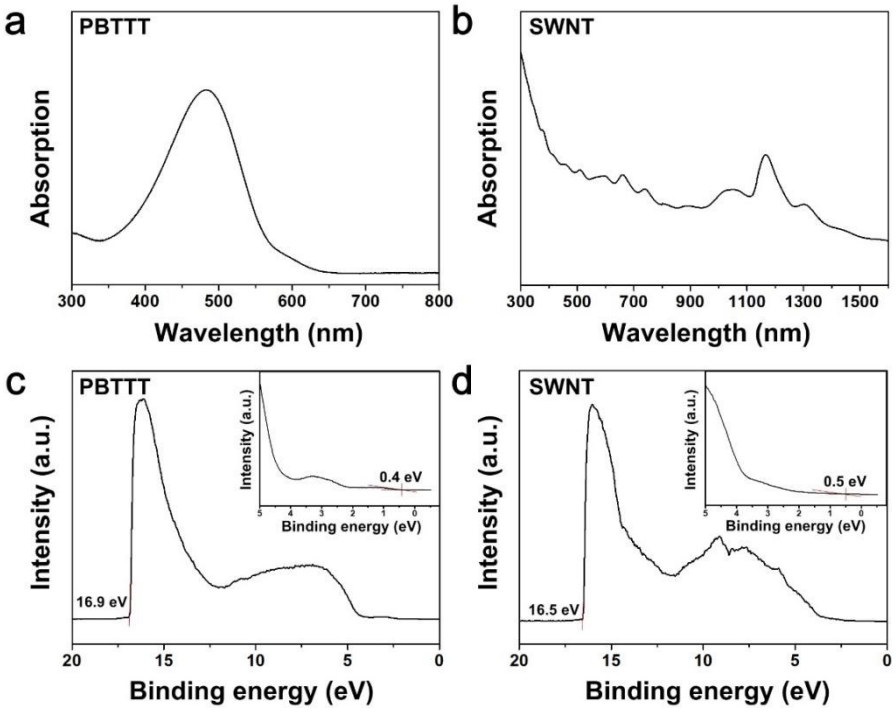

Figure S8. a,b) UV-vis-NIR optical absorption spectra of PBTTT solution in ODCB and SWCNT dispersion in DMF, respectively. c,d) Ultraviolet photoelectron spectroscopy (UPS) of PBTTT film and SWCNT film, respectively.

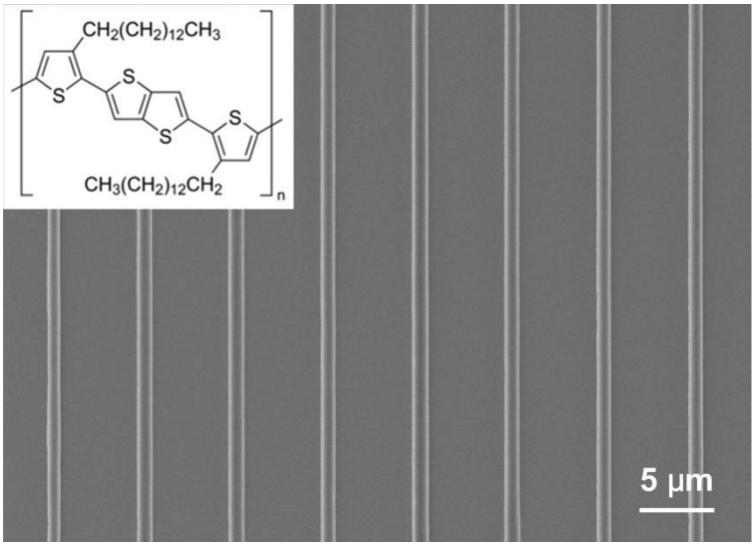

Figure S9. Top-view SEM image of the regular aligned 1D PBTTT arrays fabricated by the line-pillar structured template. Inset shows the chemical structure of PBTTT-C14.

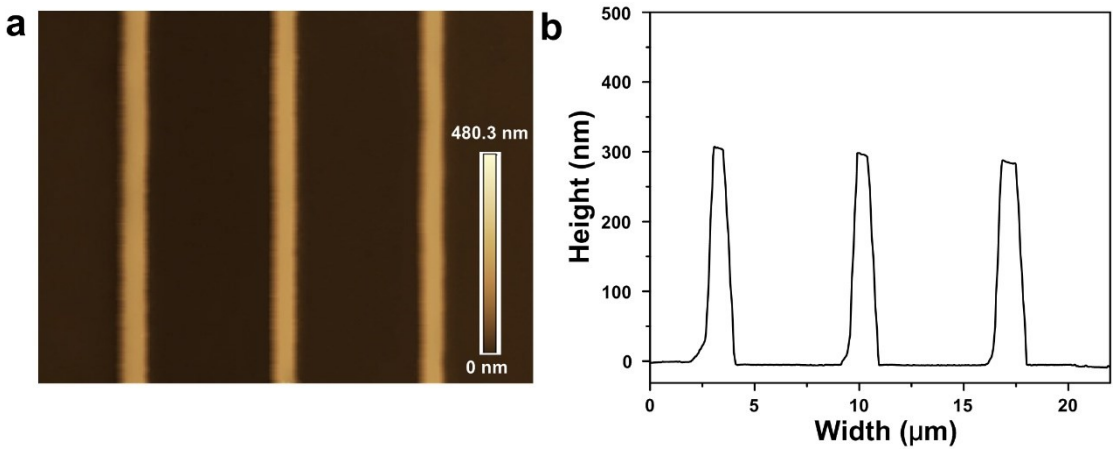

Figure S10. AFM characterization of 1D PBTTT arrays. a) AFM image of the aligned 1D PBTTT arrays. b) The height diagram displays the height of the 1D structures is *ca.* 300 nm.

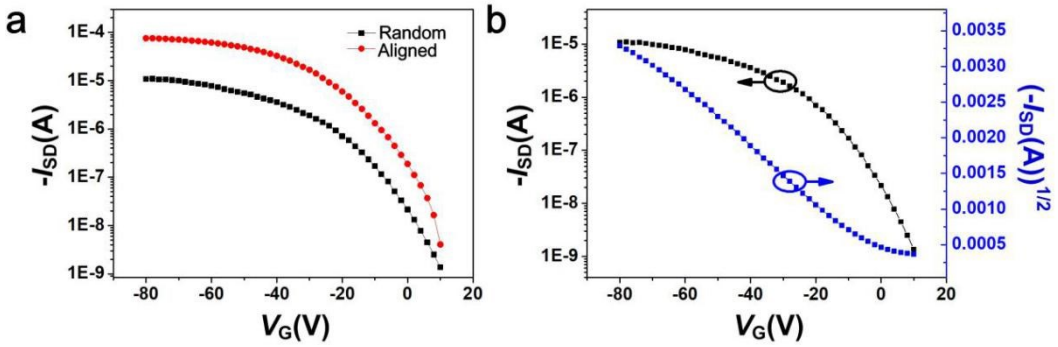

Figure S11. a) I_{SD}-V_G transfer characteristics of FETs based on random and aligned PBTTT/SWCNT network. b) Typical transfer curves of random-network PBTTT/SWCNT transistors.

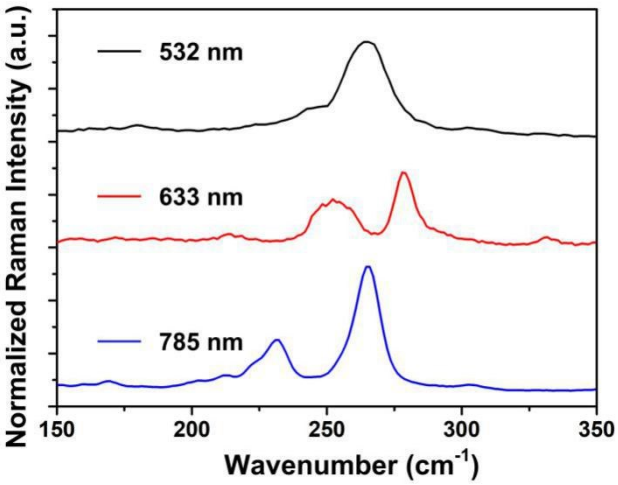

Figure S12. Raman spectra of (7,6) SWCNT under 532 nm, 633 nm, and 785 nm excitation in the radial breathing mode (RBM) region. Under the 532 nm excitation, a range of RBM peaks from 225 cm^{-1} to 298 cm^{-1} are observed, corresponding to SWCNT with diameter (d_t) ranging from 0.83 nm to 1.1 nm according to the equation $d_t = 248/\omega_{RBM}$, where d_t is diameter of SWCNT and ω_{RBM} is RBM frequency.